

#### Impact of speed planning for inland vessels with alternative power systems on energy efficiency and emissions

Slagter, Simeon; Jiang, Man; Pang, Yusong; Visser, Klaas; van Koningsveld, Mark; Negenborn, Rudy R.

DOI

10.1016/j.ecmx.2025.101223

**Publication date** 

**Document Version** Final published version

Published in

**Energy Conversion and Management: X** 

Citation (APA)
Slagter, S., Jiang, M., Pang, Y., Visser, K., van Koningsveld, M., & Negenborn, R. R. (2025). Impact of speed planning for inland vessels with alternative power systems on energy efficiency and emissions. *Energy Conversion and Management: X, 28, Article 101223.* https://doi.org/10.1016/j.ecmx.2025.101223

Important note

To cite this publication, please use the final published version (if applicable). Please check the document version above.

Copyright

Other than for strictly personal use, it is not permitted to download, forward or distribute the text or part of it, without the consent of the author(s) and/or copyright holder(s), unless the work is under an open content license such as Creative Commons.

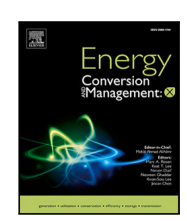
Please contact us and provide details if you believe this document breaches copyrights. We will remove access to the work immediately and investigate your claim.

FISEVIER

Contents lists available at ScienceDirect

### **Energy Conversion and Management: X**

journal homepage: www.sciencedirect.com/journal/energy-conversion-and-management-x





# Impact of speed planning for inland vessels with alternative power systems on energy efficiency and emissions

Simeon Slagter <sup>a,c</sup>, Man Jiang <sup>b,c</sup>, Yusong Pang <sup>a,c</sup>, Klaas Visser <sup>a,c</sup>, Mark van Koningsveld <sup>b,c</sup>, Rudy R. Negenborn <sup>a,c</sup>

- <sup>a</sup> Delft University of Technology Department of Maritime and Transport Technology, Mekelweg 2, Delft, 2628 CD, Netherlands
- <sup>b</sup> Delft University of Technology Department of Hydraulic Engineering, Stevinweg 1, Delft, 2628 CN, Netherlands
- c Netherlands Maritime Knowledge Center, Leeghwaterstraat, Delft, 2628 CN, Netherlands

#### ARTICLE INFO

# Keywords: Voyage optimization Non-linear control systems Energy transition Inland shipping Green hydrogen PEMFC

#### ABSTRACT

The inland waterway transport sector is facing increasingly stringent legislation to reduce emissions and improve energy efficiency. Speed planning has the potential to provide logistically compliant, energy-efficient, and emission-reducing voyages for inland vessels. However, current speed planning methods do not consider PM and  $NO_x$  emissions, nor do they consider alternative power systems to internal combustion engines (ICE) and full electric systems. These omissions have led to a lack of clarity on the impact of speed planning on the emission profile of inland vessels and the impact of alternative power systems on energy consumption. In this paper we propose a validated speed planning method that considers the emission profile ( $CO_2$ ,  $PM_{10}$ , and  $NO_x$ ) and different engine types for inland vessels in an leg-based speed planning approach while taking into account varying fairway water depth and speed. Through a use case we show that the vessel can achieve a 7.26% energy, 5.37%  $CO_2$  and fuel, 3.85%  $NO_x$ , and 6.77%  $PM_{10}$  reduction while maintaining the same arrival time; showing a distinct difference of this method compared to slow steaming. We also find that  $CO_2$ ,  $NO_x$ ,  $PM_{10}$ , and energy are not directly proportional when making speed adjustments. Finally, we analyze the adverse effects of emission control areas and emission limits on the energy consumption and arrival times of vessels with non-zero emissions propulsion.

#### 1. Introduction

#### 1.1. Background

Emissions have strong adverse effects globally and locally on health, climate, and the environment. In 2019 the European Commission launched the European Green Deal strategy to overcome climate change challenges; aiming at reducing the net greenhouse gas emissions by 55% by 2030, and to be climate-neutral by 2050 [1]. The Commission also proposes to enhance long-term energy efficiency measures, including an increase from 9% to 11.7% of the binding Energy Efficiency Target [2]. Moreover, the REPowerEU plan and Renewable Energy Directive (RED) aim to increase the 2030 target for renewables from 40% to 42.5% [3,4]. In the transport sector this legislation is enforced through the 'Sustainable and Smart Mobility Strategy' act [5].

Inland waterway transport (IWT) is one of the most CO2-efficient modes of transport in terms of tonne-kilometers and is considered vital in transitioning to sustainable transport systems in Europe [6].

However, this competitive advantage is fleeting if the sector does not take action to decarbonize and increase their sustainability quickly. To address the challenges faced by the IWT sector and deliver on the objectives of the European Green Deal and the Sustainable and Smart Mobility Strategy, the European Commission is putting forward an 'IWT Action Plan 2021-2027' [6]. The plan includes four aspects: (1) Shifting more freight transport to inland waterways; (2) Transitioning to zero-emission IWT; (3) Smart IWT; (4) Creating more attractive and sustainable jobs in IWT.

Many operational, design, retrofitting, and alternative fuel solutions have been proposed to reduce the emissions of inland shipping. A method of particular interest is voyage optimization, which is a method that aims to provide safe, energy-efficient, timely, and emission-reducing voyage planning for ships. Through voyage optimization, optimal routes and speeds are selected for which emissions are minimized and for which constraints on voyage scale are satisfied. Compared to technical and retrofitting solutions, voyage planning

E-mail address: s.slagter@tudelft.nl (S. Slagter).

<sup>\*</sup> Corresponding author.

<sup>&</sup>lt;sup>1</sup> These two authors are co-first authors with equal weighted contribution to this article.

methods are quick to implement and ensure operational continuity through little or no downtime. Voyage optimization not only reduces the emissions of ships, it can also improve the energy efficiency. In addition, voyage optimization methods contribute to the smart navigational aspect of the IWT action plan, as they can help facilitate the automation of navigational aspects of inland shipping. However, voyage planning alone is not sufficient to reach the emission and energy reduction goals of the EU; voyage planning can reduce the emissions but it cannot reduce them to zero.

## 1.2. Literature review of energy-efficient voyage optimization for inland shipping

For inland shipping there is often only one route from origin to destination. Consequently, voyage optimization for inland shipping often becomes speed planning, rather than joint speed and route planning. The speed planning methods discretize the journey into parts often called segments, stretches, stages or legs; subsequently, the optimal speed for each stretch is determined for which the objective function is minimized. Common objectives include fuel consumption, cost, and emission minimization. The discretization of the journey into segments occurs based on location or waterway characteristics. For example, journey segments can be chosen as the river segments connecting different cities along the journey [7]; therefore, each segment connects two port cities, this is often referred to as port-call planning. Alternatively, the segments are chosen based on distinctive and varying conditions of the river such as water depth, water speed, locks, bridges, or reaching a port [8,9]. Similarly, [10] segment the journey according to hydrological conditions, specifically current speed and water depth, which enables the model to better capture local resistance variations and improve the accuracy of energy-efficient speed planning. In this way, leg-based speed planning allows the ship's speed to change multiple times between ports, leading to higher resolution and accuracy compared to port-call planning; for ease of comparison we name this 'leg-based speed planning'. The benefit of leg-based speed planning is that it accounts for the changing fairway and wind conditions along the journey. Additionally, navigational aspects such as Emission Control Areas (ECAs) [11], bridges, and lock planning [12] can be easily integrated in this framework. For instance, each ECA along the journey can be represented by a single stretch for which the emissions are modeled and a suitable speed is selected. Locks can signify the beginning or end of a leg, in this fashion waiting times can be easily modeled in between two legs.

Some speed planning methods consider the environmental conditions such as the water depth, current, and wind. These environmental conditions lead to a significant increased accumulated additional resistances through the shallow water effect, currents and wind resistances. The vessel speed also influences these resistances, therefore, ideally these factors are taken into account in the speed plan. For instance, the Holtrop & Mennen resistance models are supplemented by wave and wind resistance models to take into account the different environmental conditions acting on the ship in [8]. The segments are determined based on waterway conditions using a k-means clustering algorithm. Subsequently, the speed planning is determined for three different ships in dry and rain season. Speed planning for a fleet of inland vessels while considering water depth, water speed and wind conditions is proposed by [9]. Another study addresses fleet-level decision making by jointly considering the adoption of green technologies and ship deployment for inland vessels under speed limits and varying currents, offering insights for policymakers [13].

Other papers, rather than focusing on improving the utility of the models have sought to improve the optimization process by applying novel methods, a shuffled frog-leaping algorithm in [14], and an augmented Lagrangian differential evolution algorithm [15]; they successfully show that by using these methods a better solution is found compared to particle swarm optimization, which is commonly used to

solve the speed optimization problems [8,9]. A dynamic programming model is used to find the optimal speed setpoints for a leg-based speed planning method in [7]. The method includes the current speeds on different segments but not other environmental states.

Some methods only consider the navigational conditions of the ship, ship specifications and maneuvering [12,16]. These methods often focus on a novel speed planning aspect but forego the detailed modeling of resistances and consideration of fairway conditions. For instance, the lock scheduling of ships is modeled for inland waterways under uncertainty and subsequent speeds are selected to minimize fuel consumption and CO<sub>2</sub> emissions in [12]. In contrast, the coordinated scheduling of multiple vessels passing through a series of locks — including those on tributaries - has been shown to improve overall efficiency and reduce emissions [17]. The effects on speed planning by utilizing green fuels and scrubber installations for emission reductions are considered by [16]. Complementary to these studies, alternative power system solutions such as battery and hybrid propulsion have been assessed for inland ships, with life-cycle environmental and economic impacts evaluated under carbon pricing scenarios and uncertainty analysis [18]. A speed optimization problem for which either costs or emissions are minimized, and the effects of carbon tax on speed planning is considered by [19].

Voyage optimization can also be combined with energy management systems leading to joint speed and energy optimization. These combined methods are developed for battery-powered all-electric ships where a non-linear ship energy and speed optimization model is established and the optimal speed per segment, and departure times can be found using a non-dominated sorting differential evolution algorithm [20,21]. The benefit is that in the voyage plan, the energy transfer required from the engines is already considered, leading to a more accurate speed planning and improving the overall energy efficiency of the ship. The integration of energy management systems with speed planning methods becomes more difficult for hybrid propulsion systems. Additionally, speed can be co-optimized with trim to further reduce fuel consumption and emissions, as trim adjustments influence the resistance and propulsion efficiency of the vessel [22].

Almost all of the literature available on the topic of energy-efficient speed planning is developed specifically for sea-going vessels or shortsea shipping. In contrast, speed planning developed for inland vessels can be considered under-explored as relatively few works have been published on this topic. What is currently still missing in literature is: Firstly, methods that consider more than CO<sub>2</sub> and SO<sub>3</sub> emissions, namely, also particulate matter (PM), and nitrogen oxides (NO<sub>x</sub>). It is important to consider these emissions as they can have a significant impact on the health of people in high density transport areas [23]. The quantification of these emissions for segments of inland waterways have already been published in [24-26]. However, these models have not yet been leveraged for the purposes of speed planning nor has impact of speed selection on emissions been clearly identified. Secondly, methods that consider speed planning for ships with different power systems such as fuel cells and the effects of these alternative power systems on energy efficiency; it is imperative to know and understand this effect during and after the energy transition. Through a speed planning method that considers CO2, PM, and NOx emissions and alternative power systems we can also assess the impact of legislative initiatives such as ECAs, emission limits and carbon tax. Thirdly, safe speed planning for low navigable waters has not been considered. Many works consider water depth as a parameter and [8] even considers the dry season of its use case river. However, what is missing is a speed planning that takes into account the squat-effect of the vessel and through constraints ensures that a suitable speed is selected for which the ship does not ground in low-navigable waters. Fourthly, a visualization of the solution space of speed planning and its relationship to various Key Performance Indicators (KPI) such as emissions, fuel consumption, fuel cost, energy, and travel time. Through this visualization ship owners and captains can better understand the speed choices and sailing strategies.

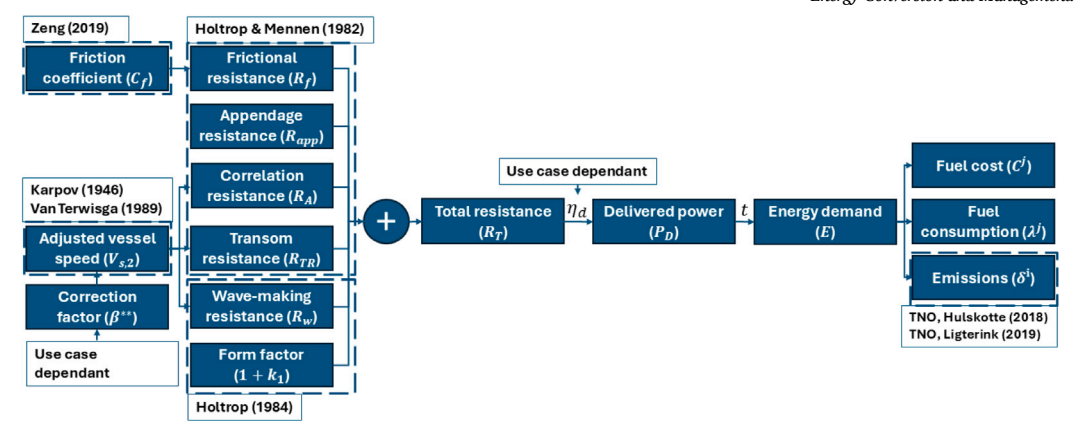


Fig. 1. The relationships between resistance, power, energy and performance indicators and their respective sources. The required inputs to apply this method are shown in Table 1, they include vessel characteristics, engine & powertrain specifics, emission parameters and waterway information per leg.

#### 1.3. Aim & contribution

The effects of speed planning on energy efficiency for inland vessels with different power systems is not known. Additionally,  $\mathrm{NO}_x$  and PM emissions are not considered in the speed planning methods that have been established for inland shipping, even though inland vessels often operate near urban areas. For that reason, our aim is threefold: 1. Clarify the impact of speed planning on the emission profile ( $\mathrm{CO}_2$ , PM, and  $\mathrm{NO}_x$ ) of inland vessels and to visualize the solution space so that captains and ship owners can make better informed sailing strategies; 2. Evaluate the impact of alternative engine types on the total energy consumption and fuel costs; 3. Assess the impact of different legislative initiatives such as ECAs, emission limits and carbon tax on the energy, emissions and fuel costs performance of inland vessels.

Specifically, in this paper we illustrate the capabilities of our speed planning models using two principally different conversion systems. On the one hand, internal combustion engine (ICE) related conversion of fossil fuels with intrinsic  $\mathrm{CO}_2$ ,  $\mathrm{NO}_x$ , and PM emissions and on the other hand, electrochemical hydrogen conversion in proton exchange membrane fuel cells (PEMFC) with zero emissions. We evaluate and compare the energy efficiency performance of vessels with these conversion systems, while taking into account environmental conditions of the river such as water depth and water speed. Additionally, the two conversion systems are used to highlight differences in speed planning under future potential legislation of emission caps and emission control areas.

The research novelty is the development of a speed planning model that models the emission profile ( $\mathrm{CO}_2$ , PM, and  $\mathrm{NO}_x$ ) and considers different engine types for inland vessels in a leg-based speed planning approach while taking into account the fairway conditions. Therefore, the speed planning method presented in this paper can also be used to evaluate other engines and fuels that are key to transitioning to zero-emission inland waterways, such as green ammonia and green methanol.

#### 1.4. Structure of the paper

The speed planning model is given in Section 2 in which we describe the resistance models of inland ships in shallow waters and relate the resistance to various key performance indicators such as power, energy, the emission profile, fuel and costs. Consequently, we define a use-case and validate the models in Section 3. Thirdly, we exemplify the use of the models through a study of scenarios and discuss their results in Section 4. Finally, we draw conclusions and recommend future work in Section 5

#### 2. Leg-based speed planning model

The speed planning model we present in this paper is leg-based. The journey from origin to destination is discretized into segments

based on distinctive waterway characteristics such as water depth and current velocity. The aim of the speed planning model is to find the optimal speed for each leg of the journey for which the overall energy consumption of the ship is minimized. For each leg of the journey the resistance, energy and emissions of the ship has to be calculated, therefore the models described below are all a function of the leg of the journey. The speed planning model can be divided into three parts, namely: 1. the resistance models of a ship in shallow waters; 2. the energy and emissions models; 3. the objective function and constraints on ship squat, vessel speed and arrival time that define the optimization problem. The relationships between resistance, power, energy and performance indicators are shown in Fig. 1.

#### 2.1. Resistance modeling of an inland ship in shallow waters

We use the open source models of OpenTNSim-Energy [27], which is built upon the Open source Transport Network Simulation (OpenTNSim) [28], to model the ship's resistance in shallow waters. The approach can be summarized in the following steps: 1. Use the Holtrop and Mennen [29] resistance models for open water; 2. Apply Zeng's correction on the frictional coefficient  $C_f$  for shallow water [30]; 3. Use Holtrop's form factor to take viscous resistance into account [31]; 4. Apply the Karpov method [32,33] for velocity corrections of a ship in shallow waters, which influence the wake, transom, and model correlation resistances; 5. Apply a correction to the Karpov method because it tends to overestimate the resistance on ships in shallow water under certain conditions of draft and water depth. This correction  $(\beta^{**})$  is tuned on a use-case basis and, within each use case, varies as a function of water depth. Steps 1-5 are described mathematically below. For the sake of brevity, the parameters that do not deviate from the Holtrop and Mennen models will not be repeated in this paper; only the corrections will be elaborated.

The Holtrop & Mennen method provides a transparent resistance decomposition for conventional displacement hulls in deep-water conditions. To extend its applicability to inland navigation, we include two corrections that address the dominant shallow-water mechanisms described by [34]: 1. Zeng's correction for the hydraulic effect, the increase in viscous resistance caused by restricted waterway cross-section (limited depth and width), and 2. the Karpov method for the undulatory effect, the local flow acceleration in shallow waterways that amplifies wave-making resistance. As noted by [35], extending deepwater models in this way can introduce estimation errors compared with resistance formulations developed specifically for shallow or confined waters. In our case, this drawback is mitigated by calibrating the resulting speed–power curves against measurements, which ensures reliable resistance estimates for our vessel with a block coefficient of 0.85 operating at depth-to-draft ratios of  $h_n/D_s \geq 1.5$ .

We choose a modeling approach, instead of a data-driven approach, to estimate the resistance of the ship to ensure a wide applicability of the method. The method can be used for a broad range of vessel dimensions, vessel draft, water depths and currents. The same is difficult to achieve with a data-driven approach and limited data. Therefore, the benefit of the model approach is that users can still apply the speed planning method by using some assumptions in case there is little or no data available. This will allow them to get an indication of how speed planning and alternative engines will affect the performance of their use case.

Step 1. The Holtrop and Mennen [29] resistance models stated in equation 1, show that the total resistance of a ship  $(R_T)$  in [N] is the sum of the frictional resistance  $(R_f)$ , wave-making and wave-breaking resistance  $(R_w)$ , resistance of the appendages  $(R_{app})$ , resistance due to immersed transom  $(R_{TR})$ , resistance of the bulbous bow near the water surface  $(R_R)$ , and model–ship correlation resistance  $(R_A)$ .

$$R_{T}^{n} = R_{f}^{n} \left( 1 + k_{1} \right) + R_{w}^{n} + R_{app}^{n} + R_{TR}^{n} + R_{A}^{n} + R_{B}^{n} \quad \forall \quad n \in \mathbb{N}$$
 (1)

In the speed planning model the resistance on each leg n of the journey has to be calculated separately. The set of n legs is N.

$$N = \{1, 2, 3, \dots, n\} \tag{2}$$

The frictional resistance of the ship is calculated using the Holtrop & Mennen formulation:

$$R_f^n = \frac{1}{2}\rho(V_s^n)^2 C_f^n S \quad \forall \quad n \in \mathbb{N}$$
 (3)

in which  $\rho$  is the density of water [kg/m³];  $V_s$  is the speed of the vessel over water [m/s];  $C_f$  is the friction coefficient; S is the wetted surface area of the hull [m²].

Step 2. To model the friction coefficient for a vessel in shallow waters as accurately as possible we use the method proposed by Zeng [30]. This approach adjusts the friction coefficient to take into account the additive friction resistance below the ship in shallow waters; Mathematically:

$$C_f^n = C_{f0}^n + (C_{f,shallow}^n - C_{f,Katsui}^n) \frac{S_B}{S} (\frac{V_s^n + \Delta V_n}{V_s^n})^2 \quad \forall \quad n \in \mathbb{N},$$
 (4)

in which  $C_{f0}$  is the frictional resistance curve as agreed on by the ITTC [36];  $C_{f,Katsui}$  is Katsui's friction coefficient for a flat plate in unrestricted water [37];  $C_{f,shallow}$  is the frictional coefficient for a flat plate in shallow waters derived through CFD models [30];  $S_B$  is the area of the flat bottom of the ship  $[m^2]$ ;  $V_s + \Delta V$  is the increased velocity underneath the ship's bottom [m/s]. The velocity underneath the ships bottom is calculated according to Zeng's method:

$$V_s^n + \Delta V_n = 0.4277 \cdot V_s^n \cdot \exp\left(\frac{h_n}{D_s}\right)^{-0.07634} \quad \forall \quad n \in \mathbb{N}$$
 (5)

The reported uncertainty of this formula is 2.5% [30], and it is only suitable for  $\frac{h_n}{D_s} \leq 4$ ;  $D_s$  is the draft of the ship. For  $\frac{h_n}{D_s} \geq 4$ ,  $V_s^n + \Delta V_n$  is assumed to be equal to  $V_s^n$  [25].

Step 3. The viscous resistance of the ship is taken into account through a form factor. We use the form factor proposed by Holtrop [31]:

$$1 + k_1 = 0.93 + 0.487c_{14} \left(\frac{B_s}{L_s}\right)^{1.068} \left(\frac{D_s}{L_s}\right)^{0.461} \left(\frac{L_s}{L_R}\right)^{0.122} \left(\frac{L_s^3}{\nabla}\right)^{0.365} \left(1 - C_P\right)^{-0.604},$$

in which  $c_{14}$  is a coefficient accounting for the stern shape [–];  $C_P$  is the prismatic coefficient based on the waterline length [–];  $B_s$  is the beam of the ship [m];  $L_s$  is the ship's length at the waterline [m];  $\nabla$  is the ship's water displacement [m³];  $L_R$  is a length parameter [m] and is estimated using the Holtrop and Mennen method [29].

Steps 4 and 5. In shallow waters as the vessel speed increases the height of the produced waves increases also, which results in an increased wave-making resistance compared to deep water conditions. To take this effect into account we determine the Froude number:

$$Fr_L^n = \frac{V_{s,2}^n}{\sqrt{gL_s}} \quad \forall \quad n \in \mathbb{N}$$
 (7)

in which  $V_{s,2}$  is the adjusted vessel speed taking into account the real velocity underneath the ship's bottom according to the work of [32,33]. The adjusted speed is calculated using:

$$V_{s,2}^n = \frac{\beta^{**} \cdot V_s^n}{\alpha^{**}} \quad \forall \quad n \in \mathbb{N},$$

$$\tag{8}$$

in which  $\alpha^{**}$  is an empirical parameter that can be estimated using the Froude number calculated with the original speed, and the ratio of water depth and draft [25]. This method is an application of the Karpov method [32], exemplified in [24]. This Karpov method is an approach that overestimates the vessel speed at lower water depths leading to an overestimation of resistance. For that reason, we apply a correction  $(\beta^{**})$  to the estimated adjusted vessel speed. This correction factor can be chosen as a function of water depth and use-case characteristics.

Subsequently, the Froude number with adjusted speed  $(Fr_L^n)$  is used to determine the wave-making and wave-breaking resistance  $(R_W)$  according to Holtrop [31]. Holtrop proposes three different wave resistance models for varying Froude numbers through which the wave resistances can be estimated more accurately for different speed ranges. The adjusted speed  $(V_{s,2}^n)$  is used to determine the transom resistance  $(R_{TR})$  and appendage resistance  $(R_{qpp})$ .

Finally, for inland vessels a few assumptions can be made: 1. Most inland ships do not have a bulb [25], naturally this leads to a resistance of the bulbous bow of zero,  $R_B = 0 \ \forall \ n \in \mathbb{N}$ ; 2. Most inland vessels have a relatively high block coefficient because they maximize cargo space. Therefore, we assume that the block coefficient is  $C_B = 0.85$  which is the maximum value for which the Holtrop and Mennen [29] method is applicable; 3. The afterbody form of the ship has a normal section shape, leading to  $c_{14} = 1$  [31]; 4. An average appendage resistance factor of 1 + k2 = 2.5, which is consistent with suggested values in the Holtrop and Mennen work [29].

#### 2.2. Energy and emissions modeling

To evaluate the speed plan we model various Key Performance Indicators (KPI) and relate them to the total ship resistance and speed. The KPI we model are power, energy, emissions, fuel consumption, fuel cost, and travel time. We can relate resistance to power with the following:

$$P_D^n = \frac{R_T^n \cdot V_s^n}{\eta_d^n \cdot 1000} \quad \forall \quad n \in \mathbb{N}, \tag{9}$$

in which  $P_D$  is the power delivered to the propeller [kW], which is estimated by taking into account the hydrodynamic efficiency of the ship,  $\eta_d$ . The hydrodynamic efficiency can be calibrated specifically for the use case and as a function of water depth. The energy demand at the propellers [kWh] for stretch n is  $E_n$ :

$$E_n = P_D^n \cdot \frac{d_n}{3600V_{op}^n} \quad \forall \quad n \in \mathbb{N}, \tag{10}$$

in which  $\frac{d_n}{3600V_{og}^n}$  is the sailing duration [h] on stretch n, and can be estimated by relating distance traveled (d) [m] and speed over ground ( $V_{og}$ ). The total energy demand at the propellers of the ship during the trip ( $E_{trip}$ ) [kWh], is the sum of the energy demand on the stretches ( $E_n$ ); similarly, the total travel duration,  $t_{trip}$  [h], is the sum of the travel duration on each stretch n.

The speed over ground can be inferred by the ship speed and current velocity,  $V_c$  [m/s]. In this formula the current direction is taken as

positive when flowing in the same sailing direction as the ship.

$$V_{\alpha g}^{n} = V_{s}^{n} + V_{c}^{n} \quad \forall \quad n \in \mathbb{N}$$

$$\tag{11}$$

The expected fuel consumption [tonne] on leg n for engine type j can be estimated using [38]:

$$\lambda_n^j = \frac{E_n \beta_n^j}{\rho_{_L}^j \eta_{_L}^j} \quad \forall \quad n \in \mathbb{N}, j \in J,$$
(12)

in which  $\beta_n^j$  is the partial engine load correction factor [–]. The engine load  $L_f^n$  is explicitly calculated for each edge as:  $L_f^n = \frac{\rho_D^n}{\eta_g \eta_t} \cdot \frac{100}{\rho_{max}}$ , where  $\rho_D^n/(\eta_g \eta_t)$  is the engine brake power on edge n (derived from delivered power, vessel speed, resistance, and propulsive efficiency),  $\rho_{max}$  is the maximum rated engine power, and  $\eta_g$  and  $\eta_t$  are the gearing and transmission efficiencies respectively [–]. This ensures that the load reflects the vessel's actual operating condition on each route segment. Based on this computed load percentage, we look up the corresponding correction factor  $\beta_n^j$  from reference datasets: [39] for internal combustion engines and [38] for fuel-cells, ensuring that fuel consumption remains explicitly load-dependent.  $\rho_f^j$  is the fuel density [kWh] of the fuel used corresponding to engine j, and  $\eta_c^j$  is the overall energy conversion efficiency covering the powertrain before the propellers for each associated powertrain relating to engine j; J is a set of engine types that can be evaluated using the speed planning models provided in this paper.

$$J = \{Engine \ type \ 1, Engine \ type \ 2, \dots, Engine \ type \ j\}$$
 (13)

The associated fuel costs  $C_n$  [euro] are simply the multiplication of fuel price,  $p_i$  in [euro/tonne], and fuel consumption:

$$C_n^j = \lambda_n^j p_j \quad \forall \quad n \in \mathbb{N}, j \in J$$
 (14)

The total fuel consumption of the trip  $(\lambda_{trip} \text{ [tonne]})$  and total fuel costs for the trip  $(C_{trip})$  are the sums of the leg-wise fuel consumption  $\lambda_n^j$  and leg-wise fuel costs of all stretches  $n \in N$ , respectively. The final KPIs that we define are emissions. We use a method presented by the Netherlands Organisation for Applied Scientific Research (TNO) [40] in which energy consumption is related to different emission types i:

$$\delta_n^i = \frac{E_n}{\eta_n \eta_t} \cdot \delta_f^i \cdot \delta_{correction}^{i,n} \quad \forall \quad n \in \mathbb{N}, i \in I,$$
 (15)

in which  $\delta_n^i$  is amount of emissions of emission type i [g];  $\delta_f^i$  is the emission factor for emission type i in [g/kWh] estimated through values reported per engine type me [39,40], and  $\delta_{correction}^{i,n}$  is the partial engine load correction factors for leg n and emission type i [40]. Therefore, this method takes into account that different engine settings leading to different emission patterns for  $\mathrm{CO}_2$ ,  $\mathrm{NO}_x$  and  $\mathrm{PM}_{10}$ ; I is the set of emissions and is defined by:

$$I = \{CO_2, PM_{10}, NO_x\}$$

$$(16)$$

These emissions are applicable in case of engine type j being an internal combustion engine. However, if for instance j is a proton exchange membrane fuel cell, then the emissions are assumed zero. The total emissions over the trip  $(\delta^i_{trip})$  is the sum of the leg-wise emissions  $(\delta^i_n)$ .

#### 2.3. Objective function and constraints

Constraints are applied on the state and decision variables which may be selected by end-user preference. Upper- and lower-bounds are set on the KPI trip-wise fuel cost, fuel consumption, emission types, travel time, and energy consumption:

$$\underline{KPI}_{trip} \le \underline{KPI}_{trip} \le \overline{KPI}_{trip}$$
 (17)

Constraints on the minimum and maximum speed over ground are imposed also. These bounds take into account the physical restriction on speed given the installed engines and water depth, and speed

limits on fairways. A maximum limit on the speed is also imposed by calculating the squat effect  $(z_n)$  [m] of the ship, and aiming to maintain a minimum clearance between the ship and the bottom of the fairway. The maximum squat is calculated with [41]:

$$z_n = \frac{C_B \cdot S_n^{0.81} \cdot (V_s^n)^{2.08}}{20} \quad \forall \quad n \in \mathbb{N}$$
 (18)

in which  $S_n$  is the blockage factor on edge n denoting how much of the cross-sectional area of the waterway is taken up by the cross-sectional area of the submerged vessel. Mathematically this is:

$$S_n = \frac{B_s \cdot D_s}{b_n \cdot h_n} \quad \forall \quad n \in \mathbb{N}$$
 (19)

where  $b_n$  is the waterway width. The constraint relating squat to vessel speed is:

$$h_n \ge D_s + z_n + \lambda \quad \forall \quad n \in \mathbb{N}$$
 (20)

In which  $\lambda$  is the prescribed minimum distance of safety [m] between the bottom of the ship and the riverbed. Therefore, the constraint enforces that there is always a minimum clearance between the ship and riverbed taking the draft and squat of the ship into account. Since  $z_n$  grows with vessel speed, Eq. (20) effectively defines an upper bound on  $V_s^n$ , reducing the feasible speed in shallow waterways. The vessel speed constraints are given by:

$$V_{s,min}^n \le V_s^n \le V_{s,max}^n \quad \forall \quad n \in \mathbb{N}$$
 (21)

The objective function has the form and aims to minimize the total energy consumption of the trip:

$$\min_{\overline{u}} J = \sum_{n=1}^{N} E_n \tag{22}$$

where  $\overline{u}$  represents the set of decision variables of the problem formulation. It should be noted that any KPI such as trip-wise fuel cost, fuel consumption, total emissions per emission type and travel time can be chosen as the minimization objective.

$$\bar{u} = \begin{pmatrix} V_s^1 \\ \dots \\ V_s^n \end{pmatrix} \tag{23}$$

The optimization problem is a constraint non-linear optimization problem, including a non-linear constraint, Eq. (20), which is a function of the decision variables. To solve the optimization problem a sequential quadratic programming approach with a multi-start procedure can be applied to ensure the global optimum is found. The threads of the multi-start method use different initial solutions and converge either to a local or global optimum; consequently, the best solution is selected. However, to give more insight in the optimization problem we have applied an alternative method, namely we choose to increment the set of decision variable values with 1.8 km/h (1 knot) and compute all solutions for all combinations of speed setpoints. This approach allows us to visualize not only the results but the whole solution space and the relationships between KPI, see Fig. 4.

#### 3. Use-case and validation

To exemplify the method presented in the previous chapter and to validate the approach we study a use-case. The Herso 1 is a CEMT class IV inland freight vessel sailing upstream from Linz (Austria) to Regensburg (Germany) for a total distance of 244 km. The speed planning method determines the appropriate vessel sailing speed on each of the legs of the journey, for which all imposed constraints are satisfied and energy consumption is minimized. By determining the vessel speed per leg, we can ensure the energy efficiency over the journey is achieved while considering the varying conditions of water depth and currents locally. The navigation circumstances of passing locks and vessel crossing are not considered in this framework. The

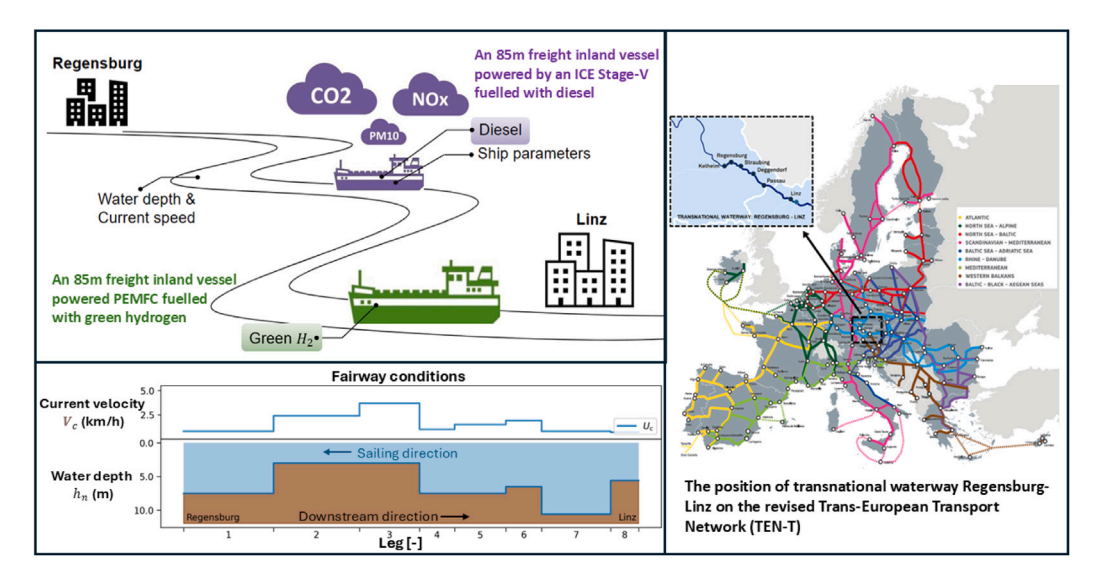


Fig. 2. Graphical overview of the use-case scenario including the fairway conditions, engine types and the position of the transnational waterway Regensburg-Linz on the revised Trans-European Transport Network (TEN-T). TEN-T image retrieved from [42].

The relationship between delivered power  $(P_D)$  and vessel speed relative to water  $(V_D)$  of the Herso 1

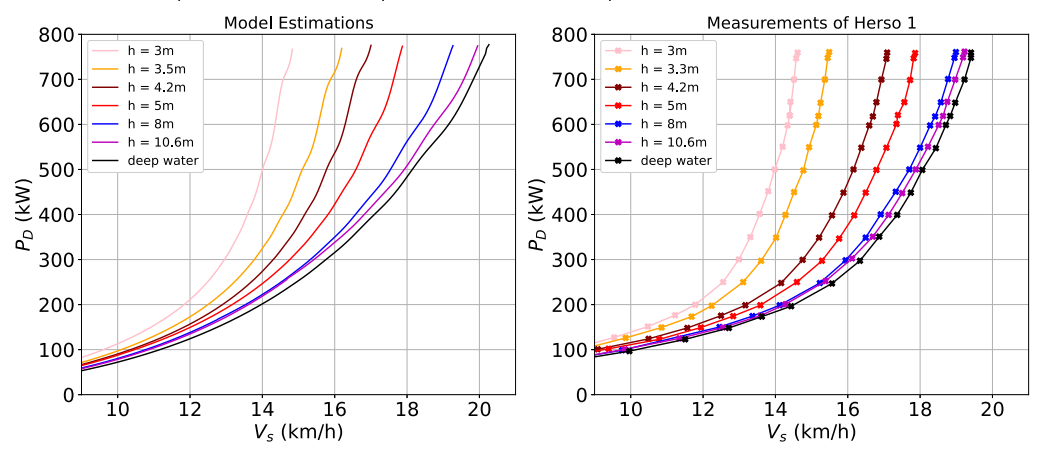


Fig. 3. The power–speed curve in of the ship in different water depths h for  $V_s \in [9, 20]$  km/h. (a) model estimation results, (b) full scale measurements. Source: Data from Schweighofer & Suvacarov [43,44]

energy efficiency is scoped for main engine propulsion only, as was already reflected in the model setup.

All the relevant journey, ship, engine, powertrain, and emission parameters of the use-case are summarized in Table 1. The use-case is the same as studied in the paper by Schweighofer and Szalma [44], as the vessel is considered representative for the Danube. The Herso 1 is powered by a conventional Stage-V diesel internal combustion engine (ICE). However, in this work we assume that the Herso 1 can also be operated using a green hydrogen fueled proton-exchange membrane fuel cells (PEMFC). We do not consider a hybrid mode in this work; the ship uses one type of propulsion throughout the journey. For that reason, the vessel with PEMFC can be considered as a second separate use-case. We assume that the loading rate and draft is the same for both cases (see Fig. 2). The chosen journey is part of the revised Trans-European Transport Network (TEN-T), and both Regensburg and Linz are core multi-modal logistics platforms. This cross-border waterway plays a key role in the Rhine - Danube Corridor, Western Balkan European Corridor, and Central European H2 corridor. We divide the journey in 8 distinct legs each with their own length  $(d_n)$ , water depth  $(h_n)$  and current velocity  $(V_C^n)$ . We study the case of low water levels, because these are of particular interest due to the climate change induced persistence of low water levels in the Danube. Additionally,

this case has not been studied before for speed planning for inland vessels.

We make a few assumptions for the use case namely: 1. An energy conversion efficiency  $(\eta_c^l)$  of 0.38 and 0.45 for the ICE and PEMFC respectively [39,45]; 2. A fuel energy density  $(\rho_f^l)$  of 11.67 and 33.30 kWh/tonne for diesel and green hydrogen fuel respectively; 3. A gearing and transmission efficiency of 0.96 and 0.98; 4. A hydrodynamic efficiency between 0.35 and 0.5 as a function of the water depth which is chosen to specifically reflect the operational data of the Herso 1; the range is considered normal for inland vessels [46,47]; 5. A fuel price in euros per tonne of 1882 and 8000 for diesel and green hydrogen, respectively [48]. The green hydrogen price is chosen in accordance with the Hydrogen Valleys platform; 6. Emission factors in g/kWh of 603, 0.015, and 1.8 for CO<sub>2</sub>, PM<sub>10</sub>, and NO<sub>x</sub> respectively [39,40]. 7. We have assumed a constant waterway width  $(b_n)$  of 150 [m].

The bounds on vessel speed shown in Table 1 are derived as follows. First, the operating range of vessel speed over ground in deep water without depth restriction is set based on available engine power, here [0-20] km/h. Next, for each leg the vessel squat is estimated as a function of speed, and the squat constraint (Eq. (20)) together with the prescribed minimum clearance  $\lambda=0.3$  m and local water depth defines the maximum allowable speed over ground,  $V_{og,max}^n$ . This step

**Table 1**Summary of all the use case parameters

Parameter	Variable	Value
	Journey parar	neters
Origin		Linz, Austria
Destination		Regensburg, Germany
Total travel distance [km]	$d_{trip}$	244
Waterway width [m]	$b_n$	150
Set of legs [–]	N	{1, 2, 3, 4, 5, 6, 7, 8}
Leg lengths [km]	$d_n \ \forall n \in N$	[48.25, 46.05, 32.23, 18.87, 27.4, 19.2, 37, 15]
Leg water depth [m]	$h_n \ \forall n \in N$	[7.5, 3, 3, 7.5, 7.5, 6.5, 10.6, 5.6]
Leg current velocity [m/s]	$V_c^n \ \forall n \in N$	[-0.22, -0.67, -1.02, -0.28, -0.42, -0.53, -0.22, -0.19]
	Ship parame	eters
Ship type		CEMT Class IV (M6) inland freight vessel
Length at waterline [m]	$L_s$	85
Beam [m]	$\boldsymbol{B}_{s}$	9.5
Draft [m]	$D_s$	2.0
Block coefficient [–]	$C_B$	0.85
Transom area [m <sup>2</sup> ]	$A_T$	3.8
Wetted area appendages [m²]	$S_{app}$	49.27
Appendage resistance factor [–]	1+k2	2.5
Correction factor [–]	$\beta^{**}$	0.75 for $h_n \le 3$ ; 0.85 for $3 < h_n \le 6$ ; 0.95 for $h_n > 6$
Hydrodynamic efficiency [–]	$\eta_d$	0.35-0.53
	General para	meters
Gravitational constant [m/s <sup>2</sup> ]	g	9.81
Water density [kg/m³]	ρ	1000
Kinematic viscosity of water [m²/s]	υ	$1.1384 \cdot 10^{-}6$
Wave resistance parameter [–]	d	-0.9
	Engine and powertra	in parameters
Engine type I		Stage-V Internal combustion engine (ICE)
Engine type II		Proton-exchange membrane fuel cell (PEMFC)
Set of engines	J	{ICE, PEMFC}
Energy conversion efficiency before propellers	$\eta_c^J \ \forall j \in J$	[0.38, 0.45]
Gearing efficiency [–]	$\eta_{ m g}$	0.96
Transmission efficiency [–]	$\eta_{t}$	0.98
Net energy density of fuel [kWh/tonne]	$\rho_f^j \ \forall j \in J$	[11.67, 33.30]
Fuel price [euro/tonne]	$p_j \ \forall j \in J$	[1882, 8000]
	Emission para	meters
Set of emissions	I	$\{CO_2, PM_{10}, NO_x\}$
Emission factors [g/kWh]	$\delta_f^i \ \forall i \in I$	[603, 0.015, 1.8]
	Constrain	
Minimum speed per leg [km/h]	$V_{s,min}^n \ \forall n \in N$	[6.61, 6.66, 7.18, 6.41, 7.71, 6.58, 6.26, 7.78]
Maximum speed per leg [km/h]	$V_{s,max}^n \ \forall n \in N$	[15.61, 12.06, 10.78, 15.41, 14.91, 15.58, 17.06, 14.98]
Maximum travel time [h]	$t_{trip,max}$	25
Minimum clearance [m]	λ	0.3

lowers the upper bounds in shallow stretches such as legs 2 and 3. The effect of local current is then added to obtain the maximum vessel speed  $V^n_{s,max}$ . Finally, vessel speed is discretized in steps of 1.8 km/h to visualize the solution space. The lower bounds  $V^n_{s,min}$  are obtained by decrementing from  $V^n_{s,max}$  until the lowest feasible speed is reached that still ensures a vessel speed over ground of at least 8 km/h. This procedure accounts for the combined influence of installed power, draft, squat, water depth, and current in defining the feasible speed range. Instead of determining such static bounds a priori, it is also possible to apply the squat constraint and an installed power constraint dynamically within the optimization problem itself, but here we opted for predefined bounds to improve transparency of the solution space.

#### 3.1. Validation of models

For the energy-efficient speed planning method it is important to have an acceptable estimation accuracy of the energy demand at the propellers ( $E_n$ ) for each leg of the journey. Since the energy is determined through the power delivered to the propeller at a given speed for a specific sailing duration, the model can be validated through the power–speed relationships at different water depths Fig. 3, and the accuracy of the estimated trip sailing duration with current influence Table 2. Furthermore, the estimation of delivered power and fuel

consumption is dependent on the model configuration of the energy conversion efficiencies at given engine loads. This estimation (using the same engine parameters as Herso 1) of diesel fuel consumption is validated by the trip fuel consumption report of the ship Table 2; the estimation of green hydrogen consumption is based on the validated PEMFC powertrain energy conversion efficiency according to [45], and empirical partial load correction factors [38]. The data used for validation and calibration of our models was retrieved from the scientific works of [43,44]; additionally, viadonau [49] supplied data on waterway conditions per leg, vessel configurations, and the operational profile of the ship. The calibration and validation of these models are specific to the use case.

The difference between the estimation and measurement of power demand can be attributed to various factors that have an influence on the resistance of the ship that our model does not take into account such as hull fouling, various external factors, uncertainty in the exact propulsive efficiencies, and the propeller behavior at different water depths [47]. To take these factors into account we choose a hydrodynamic efficiency ( $\eta_d$ ) between 0.35 and 0.5 as a function of the water depth. These values have been calibrated to minimize the estimation error for our use case specifically; they are also in the common hydrodynamic efficiency range for inland vessel in shallow waters [46,47].

**Table 2**Validation results on sailing duration and fuel consumption for upstream, downstream and round trips in Regensburg–Budapest corridor. The measurement data is from Schweighofer & Suvacarov [43,44].

	Sailing duration [h]		Difference [%]	Fuel consump	otion [tonne]	Difference [%]
	Estimated	Measured		Estimated	Measured	
Upstream trip	52.41	51.78	1.2	6547	6609	-0.94
Downstream trip	46.56	45.00	3.4	1797	1773	1.3
Round trip	98.98	96.78	2.3	8344	8382	-0.44

In Fig. 3 the model estimation of delivered power  $(P_D)$  is validated for different water depths. The different water depths are chosen to reflect the differences in the speed-power curves for varying water depths; however, it should be noted that our models are continuous and are not constrained to these speed-power curves for these specific water depths reported. For the speed range between 9 and 20 km/h, which is regarded as the common speed range for IWT vessels, the power-speed curve deviation between model estimation and measurement is 8.7% on average for this use case. This value is determined by comparing our model estimations with the full-scale measurements from Schweighofer & Suvacarov [43,44]. An model with an average error of 8.7% is considered a good estimation [50,51]; especially considering the power-speed curves are at different water depths which can significantly impact the estimated power. The achieved accuracy is only for this particular use case, we cannot state that similar values can be achieved for other use cases and ships.

The estimated trip sailing duration and diesel fuel consumption are within 3.4% and 1.3% deviation when compared to the real world data, respectively, as shown in Table 2. For the upstream case that we study in this paper the sailing duration deviates only 1.2%, indicating that the current influence is adequately reflected in our model. The fuel consumption estimation is less than 1% deviant from the real data. This relatively low fuel consumption error is specific to the present use case, where the deviations in sailing duration and in the speed–power estimation partly offset each other. In other operating conditions or for other vessels, these errors could equally amplify each other, leading to larger deviations in fuel consumption. Therefore, the close agreement reported here is not generalizable beyond this case study.

The emission estimations are calculated according to the validated method proposed by TNO [40]. They have reported the method to be based on a large amount of measurements for both the  $\rm CO_2$  and  $\rm NO_x$  estimation, and can be assumed to be reliable and accurate. However, the PM estimations are based on scarce measurements, complimented with estimations based on assumption. Therefore, the PM estimations are less reliable; this is unsurprising, as PM emissions are notoriously hard to measure. The method of estimating the emissions also includes a partial engine load correction factor leading to a more reliable estimation method compared to emission estimations based solely on engine type, (average) engine power or (average) engine running time.

#### 4. Results and discussion

The main benefits of our speed planning models are fourfold, namely: (i) they are able to reduce the energy consumption of the vessel through speed planning without necessarily lowering the speed, by considering the fairway conditions; (ii) evaluate the impact of speed on different emission types per leg; (iii) evaluate the impact of different engine types on the total energy consumption and fuel costs; (iv) evaluate the impact of different legislative initiatives on the energy and emission performance on ships.

To showcase these benefits we define 6 distinct scenarios; in each of these scenarios we operate the Herso 1 between Linz and Regensburg for a maximum allowable travel time of 25 h ( $t_{trip,max}=25$ ). Scenario 1 and 2 show the worst- and best-case scenarios from an energy perspective for the Herso 1 operating with an ICE and diesel fuel. Scenario 3 shows the best-case scenario from an energy perspective

where the Herso 1 is operating with PEMFC and green hydrogen. In scenario 4 a human skipper selects the speeds for the Herso 1 operating with an ICE. In scenario 5 there are emission control areas (ECAs) in the ports of Regensburg and Linz and we apply a constraint on the vessel speeds near these ports to lower the emissions ( $V_{s,max}^n = 10 \ \forall n = 1,8$ ). In scenario 6 we assume there is a legislative limit and constraint on the total trip emissions ( $\delta_{trip,max}^{CO2} = 2000, \ \delta_{trip,max}^{NOx} = 14$ ). Scenarios 5 and 6 are both operating the Herso 1 with an internal combustion engine.

While no formal MARPOL Annex VI ECAs exist for inland waterways, Scenarios 5 and 6 represent two ECA-like operational limitations. Scenario 5 models a port-area speed restriction (slow steaming) to reduce engine load, fuel use, and emissions during approach and maneuvering. Scenario 6 reflects a global tonne-kilometer emission cap for the journey. Comparable aims can be seen in current regulations, such as the EU Stage V engine standards for inland waterway vessels [52], and in port-level emission-sensitive tariff structures like those of Rotterdam, where dues are adjusted based on engine emission performance [53]. These measures in our modeling therefore represent plausible extensions of existing regulatory trends.

In Fig. 4 we graphically show the solution space of the optimization problem for the Herso 1 operating with an internal combustion engine. Each line going from left to right gives the combination of 8 speed setpoints on the 8 legs of the journey. These speed setpoints lead to a particular energy consumption, emission pattern, fuel consumption, fuel costs, and travel time. The gray lines are infeasible solutions as they do not satisfy the arrival time constraint. All the purple lines are feasible solutions. The optimal solution from an energy perspective is given in black, this is the solution to scenario 2. Scenario 1 is the worst-case scenario and is given in blue. The numerical solutions to the scenarios are described in Table 3. From the comparison of scenario 1 and 2 we can see that speed planning has a big influence on the total energy consumption and the other KPI. For the same arrival time, the total energy can be reduced from 7.88 kWh to 3.83 kWh, which is an energy reduction of 51%. The complete comparative performance between these scenarios can be found in Table 4.

Since it is unlikely that the skipper will choose these incredibly unfavorable speed setpoints shown in scenario 1 we introduce scenario 4. This scenario shows a realistic speed selection by a skipper, shown in Fig. 4 through the green solution. By contrasting the optimal solution found by our speed planning method (scenario 2) we show that compared to the skipper we are able to achieve a 7.26% energy reduction, 5.37%  $\rm CO_2$ , fuel and fuel costs reduction, a 3.85% reduction in  $\rm NO_x$ , and 6.77% reduction in  $\rm PM_{10}$ . Interestingly, the average weighed speed in scenario 2 is higher by 0.39%, yet we achieve a significant energy reduction. Therefore, we show that the proposed speed planning method is distinctly different from slow steaming; we achieve energy reductions by taking into account water depth and current — without compromising logistically on arrival times — by finding the optimal speed setpoints during the journey on the different legs.

By comparing scenario 2 (ICE) to scenario 3 (PEMFC) we learn that the speed setpoints and energy consumption are identical, see Table 3. This is unsurprising because we estimate the energy as a function of the power demand at the propellers. The power demand at the propellers is a function of the hydrodynamic efficiency, total resistance, and vessel speed. Since both scenarios have the same ship, propeller, and journey parameters, this will lead to the same energy

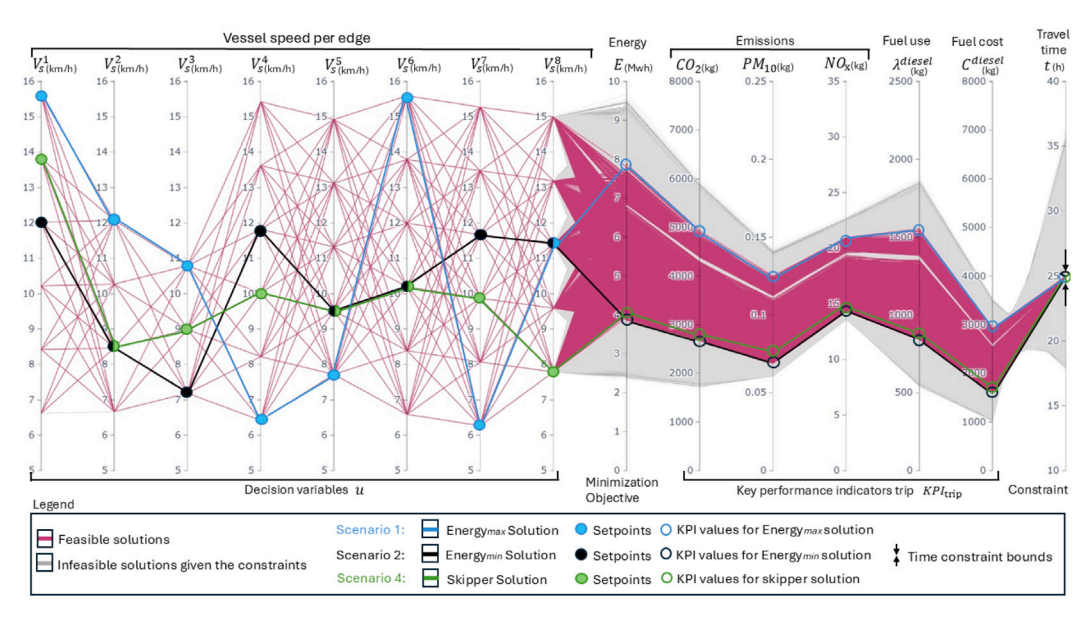


Fig. 4. The solution space of the optimization problem for a ship with an internal combustion engine and a constraint on travel time of 25 h.

**Table 3**The 6 different scenarios, their speed setpoints and resultant energy use, CO<sub>2</sub>, NO<sub>x</sub>, PM<sub>10</sub>, fuel use, fuel cost, and total travel time. Boxed values are directly effected by the constraints of that scenario.

traver time. Boxed variety are directly effected by the constraints of that section of								
Scenario	$V_{\circ}^{1}$	$V_{c}^{2}$	$V_{\circ}^{3}$	$V^4$	$V_{\circ}^{5}$	$V_{\mathfrak{s}}^{6}$	$V_{\mathfrak{s}}^{7}$	$V_{\circ}^{8}$
	(km/h)	(km/h)	(km/h)	(km/h)	(km/h)	(km/h)	(km/h)	(km/h)
1. Maximum energy use (ICE)	15.61	12.06	10.78	6.41	7.71	15.58	6.26	11.38
<ol><li>Optimal energy use (ICE)</li></ol>	12.01	8.46	7.18	11.81	9.51	10.18	11.66	11.38
3. Optimal energy use (PEMFC)	12.01	8.46	7.18	11.81	9.51	10.18	11.66	11.38
4. Skipper selects speeds (ICE)	13.81	8.46	8.98	10.01	9.51	10.18	9.86	7.78
5. ECAs in ports (ICE)	8.41	8.46	8.98	11.81	13.11	11.98	11.66	9.58
6. Emissions limits (ICE)	6.61	6.66	7.18	10.01	9.51	8.38	9.86	7.78
Scenario	Average	Energy	CO <sub>2</sub>	NO <sub>x</sub>	$PM_{10}$	Fuel	Fuel	Total
	speed	use	(kg)	(kg)	(g)	use	cost	travel
	(km/h)	(kWh)				(kg)	(EUR)	time
	(km/h)	(kWh)				(kg)	(EUR)	(h)
1. Maximum energy use (ICE)	11.02	7.88	4929.08	20.98	125.18	1553.11	2922.95	25.02
<ol><li>Optimal energy use (ICE)</li></ol>	10.17	3.83	2654.18	14.25	68.21	836.31	1573.94	24.97
3. Optimal energy use (PEMFC)	10.17	3.83	0	0	0	256.81	2054.56	24.97
4. Skipper selects speeds (ICE)	10.13	4.13	2804.86	14.82	73.16	883.79	1663.29	25.03
5. ECAs in ports (ICE)	10.13	4.15	2813.72	14.87	73.64	886.58	1668.54	24.97
6. Emissions limits (ICE)	7.99	2.78	1991.59	13.87	62.35	627.53	1181.01	31.65

Table 4
Relative energy, emissions, and fuel savings in different scenarios.

Comparison	∆Average speed (%)	∆Energy use (%)	∆CO <sub>2</sub> (%)	ΔNO <sub>x</sub> (%)	ΔPM <sub>10</sub> (%) use (%)	ΔFuel cost (%)	∆Fuel
Scenario 2 compared to 1	-7.71	-51.40	-46.15	-32.08	-45.51	-46.15	-46.15
Scenario 3 compared to 2	0	0	-100	-100	-100	-	+30.53
Scenario 2 compared to 4	+0.39	-7.26	-5.37	-3.85	-6.77	-5.37	-5.37
Scenario 2 compared to 5	+0.39	-7.71	-5.67	-4.17	-7.37	-5.67	-5.67

demand. However, taking into account the overall energy conversion efficiency covering the powertrain before the propellers  $(\eta_c^j)$  we notice a difference in fuel consumption and cost. For the fuel cell case we have a better energy conversion  $(\eta_c^{PEMFC}=0.45)$  compared to the combustion engine case  $(\eta_c^{ICE}=0.38)$ . Nevertheless, the fuel costs associated with the green hydrogen are 30.53% higher due to unfavorable prices, Table 4. In future, we expect the emission tax will raise the price of diesel fuel quickly and governments might subsidize the use of green hydrogen [54,55]. This trend could cause the fuel costs of green hydrogen to become lower than the diesel fuel cost in the next 10 to 15 years.

In scenarios 5 and 6 we consider the ideas that in the future (i) ports will have emission control areas and (ii) ships will have a maximum permissible amount of emissions over the journey, respectively. For scenario 5, we apply a constraint on vessel speed of 10 km/h on legs

1 and 8, which represent travel near Linz and Regensburg. This speed limit ensures that low emissions ( $\leq 0.25 \frac{g}{km} \ PM_{10}$  and  $\leq 0.05 \frac{kg}{km} \ NO_x$ ) are achieved around the port cities. It should be noted that in principal it is not true to say that lower speeds guarantee lower emissions; especially when considering the higher partial engine load correction factor ( $\beta^{ICE}$ ) at lower engine loads. By considering these speed constraints we can give an indication of how the energy efficiency between hydrogen powered vessels and diesel powered vessels will diverge through the imposition of ECAs. Additionally, it is common practice to lower the vessel speed around port areas. Therefore, this scenario also serves the purpose to analyze the consequences of this behavior.

In Tables 3 and 4, we show that the optimal scenario uses around 7% less energy compared to the scenario with emission control areas (ECA). This indicates that diesel powered vessels will be 7% less energy efficient compared green hydrogen powered vessels for this use

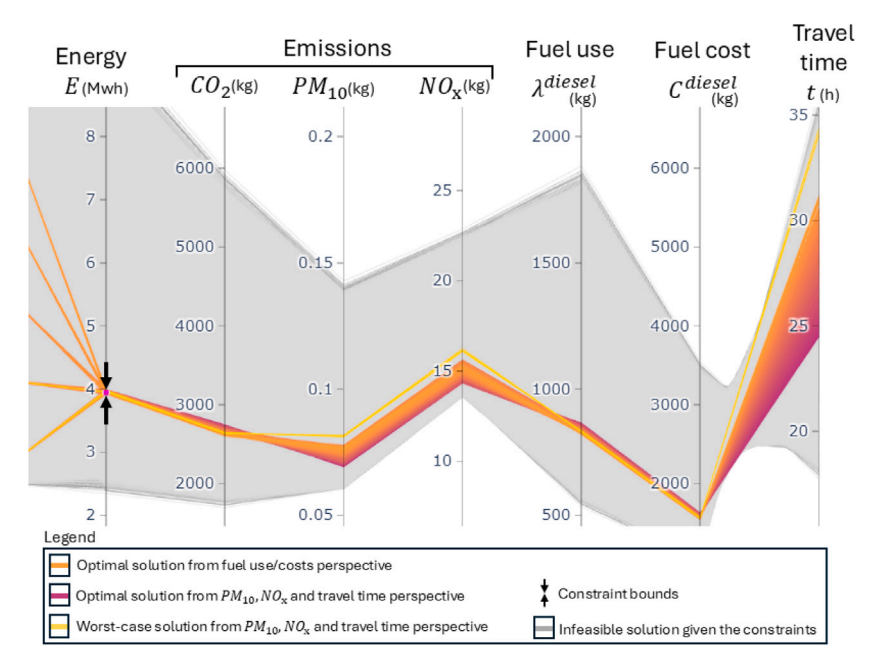


Fig. 5. The solution space of the use case with a constraint on energy consumption, highlighting the varying local relationships between emission types.

case in a future with emission control areas; since hydrogen powered vessels would not have to slow down to adhere to the ECA restrictions. Interestingly, the total emissions over the journey are lower for the scenario without ECAs with 5.67%, 4.17%, and 7.37% compared to scenario 5 with ECAs, for  $\mathrm{CO}_2$ ,  $\mathrm{NO}_x$ , and  $\mathrm{PM}_{10}$ , respectively. This is because ships tend to increase their speed outside of the ECAs to make up for lost time in the emission control areas. So although the ECAs reduce emissions locally, they could increase the emissions globally.

For scenario 6 we consider stringent emission constraints over the whole journey ( $\delta_{trip,max}^{CO2}=2000$ ,  $\delta_{trip,max}^{NOx}=14$ ). In this particular scenario it is not possible to deliver the cargo on time, in fact the ship arrives about 6.65 h late. This shows there are implications on the reliability of delivery times for non-zero emissions vessels. Therefore, these legislative initiatives steer ship owners to adopt low emission measures as these emissions constraints effect not only the energy consumption and fuel costs, but also the logistical reliability of the cargo arriving on time.

As is evident from the different scenarios, the various emissions are not linearly related. Different engine setpoints lead to varying effects on  $\mathrm{CO}_2$ ,  $\mathrm{NO}_x$ , and  $\mathrm{PM}_{10}$ ; diesel engines have different regions in their fuel maps that are favorable for the different emission types. In Fig. 5 we show this graphically where we apply a constraint on total energy consumption. We note that in orange is the optimal solution from a fuel use and costs perspective, however, from a  $\mathrm{NO}_x$ , and  $\mathrm{PM}_{10}$  perspective the solution is not near the optimum. Similarly, the purple solution is  $\mathrm{NO}_x$  and  $\mathrm{PM}_{10}$  optimal, but from the  $\mathrm{CO}_2$  and fuel perspective it is the worst-case scenario. Finally, the yellow solution is the worst-case scenario from the  $\mathrm{NO}_x$ ,  $\mathrm{PM}_{10}$  and travel time perspective but is near optimal for fuel and  $\mathrm{CO}_2$ . Because emissions do not scale directly with energy, in urban areas it would be better to use speed planning that minimize these emissions that are harmful to human health rather than the energy, fuel or  $\mathrm{CO}_2$ .

We have shown a 7% energy reduction using the proposed speed planning method. However, different use cases will lead to different energy reduction potentials. For that reason, we show a sensitivity analysis of energy consumption as a function of travel time,  $CO_2$ , fuel,  $PM_{10}$ , and  $NO_x$  in Fig. 6. We have normalized the values of the KPI between 0 and 1. From the analysis we show there is an exponential relationship between travel time and energy; as more travel time is allowed in the optimization problem, the energy consumption

decreases exponentially. This is unsurprising because travel time and speed are directly related through distance, and speed relates to resistance exponentially. The  $\mathrm{CO}_2$ , fuel use and costs are linearly related to energy.  $\mathrm{NO}_x$  and  $\mathrm{PM}_{10}$  are globally approximately linear to the energy. However, locally the slopes of the different emissions vary and will therefore show a different response in energy consumption; this is the phenomenon we showed in the scenarios and Fig. 5.

#### 5. Conclusion

To clarify the impact of speed planning on the emission profile of the ship, energy efficiency for different engine types, low navigable waters, and to assess the effect of different legislative initiatives we developed a leg-based speed planning method. Currently, the speed planning methods do not model the complete emission profile (CO $_2$ , NO $_x$ , PM $_{10}$ ), nor do they examine alternative power systems to ICE or full electric power systems. The proposed method takes these factors into account while considering the varying fairway conditions such as water depth and water speed. The models are calibrated and validated through the use-case (Herso 1) vessel sailing to and from Linz, Austria to Regensburg, Germany.

Through the study of different scenarios we show that:

- The vessel is able to achieve a 7.26% energy, 5.37% CO<sub>2</sub> and fuel, 3.85% NO<sub>x</sub>, and 6.77% PM<sub>10</sub> reduction, while achieving the same arrival time, indicating a distinct difference of the proposed method compared to slow steaming.
- CO<sub>2</sub>, NO<sub>x</sub>, PM<sub>10</sub>, and energy are not directly proportional when making speed adjustments.
- Emission control areas increase the overall emissions and energy consumption of vessels because ships will speed up outside the ECAs to maintain the desired arrival times.
- Emission caps force slow steaming on vessels resulting in arrival time constraints not necessarily being satisfied. These effects are only felt for vessels with non-zero propulsion types.
- The plans to increase carbon tax and the overall high energy conversion efficiency of fuel cells help promote the uptake of low or zero emission measures.

In future, we aim to take into account the dynamic and uncertain fairway conditions in an adaptive and robust optimization approach.

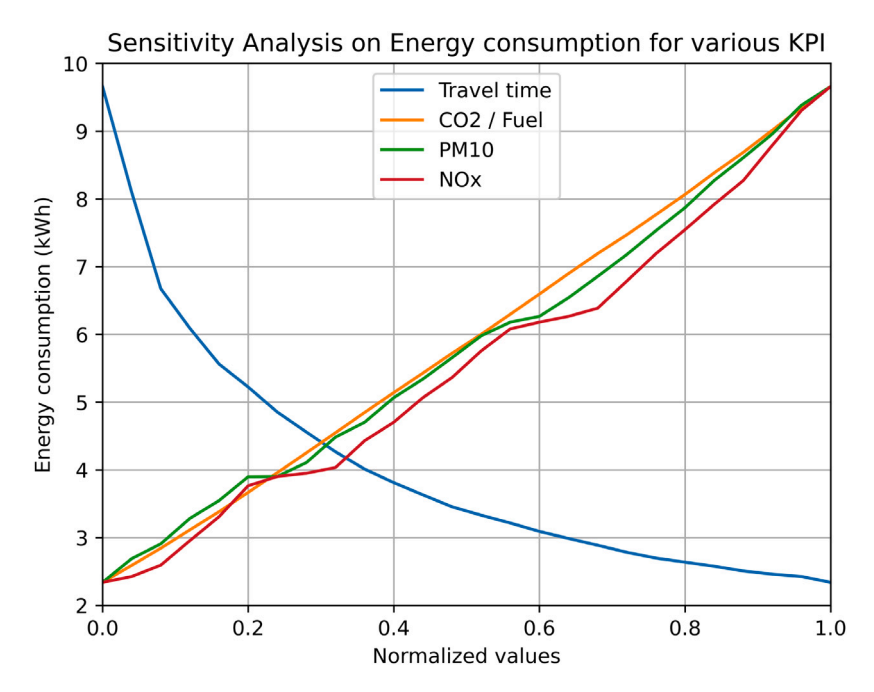


Fig. 6. Sensitivity analysis of energy consumption for varying normalized values of travel times, emissions, and fuel.

This would lead to more reliable speed planning and arrival times, and improved energy performance. Furthermore, in this work we have omitted the fact that alternative power systems require alternative bunkering strategies and that it affects the load rates of the ship. Therefore, it would be interesting to look at swapping, recharging and refueling strategies in conjunction with the speed planning for alternative power systems and fuels such as green ammonia and green methanol. Finally, we plan to compare the accuracy of different resistance models specifically developed for inland and shallow-water vessels with the adjusted Holtrop & Mennen approach used here, to better quantify model limitations and potential improvements.

#### CRediT authorship contribution statement

Simeon Slagter: Writing – original draft, Visualization, Validation, Methodology, Formal analysis, Conceptualization. Man Jiang: Writing – original draft, Visualization, Validation, Methodology, Formal analysis, Conceptualization. Yusong Pang: Writing – review & editing, Supervision, Conceptualization. Klaas Visser: Supervision, Methodology. Mark van Koningsveld: Writing – review & editing, Supervision, Funding acquisition. Rudy R. Negenborn: Writing – review & editing, Supervision, Funding acquisition.

#### Declaration of competing interest

The authors declare that they have no known competing financial interests or personal relationships that could have appeared to influence the work reported in this paper.

#### Acknowledgments

This project is supported by the NWO (Nederlandse Organisatie voor Wetenschappelijk Onderzoek), Netherlands project 'PATH2ZERO: Transition to Zero-Emission Inland Shipping' (Grant number: NWA.1439.20. 001); We acknowledge and appreciate the data support from the international waterway management organization, viadonau. The comprehensive data set provided by viadonau allowed us to calibrate and validate the models in this research paper.

#### Data availability

The data that support the findings of this study are available on request from the corresponding author, S. Slagter. The data are not publicly available due to third party ownership of the data.

#### References

- European Commission The European Green Deal. 2024, https://commission. europa.eu/strategy-and-policy/priorities-2019-2024/european-green-deal\_en.
   (Accessed 03 December 2024).
- [2] European Commission Energy Efficiency Targets. 2024, https://energy.ec.europa.eu/topics/energy-efficiency/energy-efficiency-targets-directive-and-rules/energy-efficiency-targets\_en. (Accessed 03 December 2024).
- [3] European Commission REPowerEU. 2024, https://commission.europa.eu/ strategy-and-policy/priorities-2019-2024/european-green-deal/repowereuaffordable-secure-and-sustainable-energy-europe\_en. (Accessed 03 December 2024)
- [4] European Commission Renewable Energy Directive. 2024, https: //energy.ec.europa.eu/topics/renewable-energy/renewable-energy-directive-targets-and-rules/renewable-energy-directive\_en. (Accessed 03 December 2024).
- [5] European Commission Sustainable and Smart Mobility Strategy. 2024, https://ec.europa.eu/info/law/better-regulation/have-your-say/initiatives/12438-Sustainable-and-Smart-Mobility-Strategy\_en. (Accessed 03 December 2024).
- [6] European Commission Future-proofing European inland waterway transport

   NAIADES III action plan. 2024, https://transport.ec.europa.eu/transport-modes/inland-waterways/promotion-inland-waterway-transport/naiades-iii-action-plan\_en. (Accessed 03 December 2024).
- [7] Fan A, Wang Z, Yang L, Wang J, Vladimir N. Multi-stage decision-making method for ship speed optimisation considering inland navigational environment. Proc Inst Mech Eng Part M: J Eng Marit Environ 2021;235(2):372–82. http: //dx.doi.org/10.1177/1475090220982414.
- [8] Yan X, Wang K, Yuan Y, Jiang X, Negenborn RR. Energy-efficient shipping: An application of big data analysis for optimizing engine speed of inland ships considering multiple environmental factors. Ocean Eng 2018;169:457–68. http://dx.doi.org/10.1016/j.oceaneng.2018.08.050.
- [9] Wang K, Li J, Huang L, Ma R, Qu X, Yuan Y. An Energy Efftciency optimization Methodfor Inland Ship Fleet Considering Multiple Influencing Factors. In: 2019 5th international conference on transportation information and safety. ICTIS, 2019, p. 1263–7. http://dx.doi.org/10.1109/ICTIS.2019.8883776.
- [10] Li X, Sun B, Jin J, Ding J. Ship speed optimization method combining Fisher optimal segmentation principle. Appl Ocean Res 2023;140:103743. http://dx.doi.org/10.1016/j.apor.2023.103743, URL https://www.sciencedirect.com/science/article/pii/S0141118723002845.

- [11] Wang K, Yin M, Ayisi AD. Effects of Reduced Speed on the Benefits and Pollution of Yangtze River Ships. Transp Res Rec 2023;2677(6):783–96. http://dx.doi.org/10.1177/03611981221150417.
- [12] Buchem M, Golak JAP, Grigoriev A. Vessel velocity decisions in inland waterway transportation under uncertainty. European J Oper Res 2022;296(2):669–78. http://dx.doi.org/10.1016/j.ejor.2021.04.026.
- [13] Shao S, Xu M, Tan Z, Zhen L. Ship deployment problem with green technology adoption for an inland river carrier under non-identical streamflow and speed limits. Transp Policy 2024;157:46–56. http://dx.doi.org/10.1016/j.tranpol.2024.08.003, URL https://www.sciencedirect.com/science/article/pii/S0967070X24002269.
- [14] Han C, Liu J, Liu Z, Li S, Qin X. Research on Speed Optimization of Inland Vessels Based on a Shuffled Frog-leaping Algorithm. In: 2021 6th international conference on transportation information and safety. ICTIS, 2021, p. 688–93. http://dx.doi.org/10.1109/ICTIS54573.2021.9798521.
- [15] Zhang L, Peng X, Liu Z, Wei N, Wang F. An application of augmented Lagrangian differential evolution algorithm for optimizing the speed of inland ships sailing on the Yangtze River. Int J Nav Archit Ocean Eng 2022;14:100488. http: //dx.doi.org/10.1016/j.ijnaoe.2022.100488.
- [16] Liu T. Speed optimization of inland sea vessels based on C.W saving algorithm. Appl Math Nonlinear Sci 2023;9:1–15. http://dx.doi.org/10.2478/amns.2023.2. 00271.
- [17] Zhang H, Wu Y, Jin Y, Wang S. Optimal scheduling of ships in inland waterway with serial locks. Transp Res Part C: Emerg Technol 2025;178:105241. http://dx.doi.org/10.1016/j.trc.2025.105241, URL https://www.sciencedirect.com/ science/article/pii/S0968090X25002451.
- [18] Fan A, Wang J, He Y, Perčić M, Vladimir N, Yang L. Decarbonising inland ship power system: Alternative solution and assessment method. Energy 2021;226:120266. http://dx.doi.org/10.1016/j.energy.2021.120266, URL https://www.sciencedirect.com/science/article/pii/S0360544221005156.
- [19] Tan Z, Zeng X, Shao S, Chen J, Wang H. Scrubber installation and green fuel for inland river ships with non-identical streamflow. Transp Res Part E: Logist Transp Rev 2022;161:102677. http://dx.doi.org/10.1016/j.tre.2022.102677.
- [20] Sun L, Zhang Y, Ma F, Ji F, Xiong Y. Energy and speed optimization of inland battery-powered ship with considering the dynamic electricity price and complex navigational environment. Energy Rep 2023;9:293–304. http://dx. doi.org/10.1016/j.egyr.2023.04.267, 2022 The 3rd International Conference on Power Engineering.
- [21] Zhang Y, Sun L, Fan T, Ma F, Xiong Y. Speed and energy optimization method for the inland all-electric ship in battery-swapping mode. Ocean Eng 2023;284:115234. http://dx.doi.org/10.1016/j.oceaneng.2023.115234.
- [22] Fan A, Yang J, Yang L, Liu W, Vladimir N. Joint optimisation for improving ship energy efficiency considering speed and trim control. Transp Res Part D: Transp Environ 2022;113:103527. http://dx.doi.org/10.1016/j.trd.2022.103527, URL https://www.sciencedirect.com/science/article/pii/S1361920922003534.
- [23] Aakko-Saksa PT, Lehtoranta K, Kuittinen N, Järvinen A, Jalkanen J-P, Johnson K, et al. Reduction in greenhouse gas and other emissions from ship engines: Current trends and future options. Prog Energy Combust Sci 2023;94:101055. http://dx.doi.org/10.1016/j.pecs.2022.101055.
- [24] Segers L. Mapping inland shipping emissions in time and space for the benefit of emission policy development: a case study on the rotterdam-antwerp corridor. (Ph.D. thesis), Delft, The Netherlands: Delft University of Technology - Faculty of Civil Engineering and Geosciences; 2021, URL https://resolver.tudelft.nl/uuid: a260bc48-c6ce-4f7c-b14a-e681d2e528e3.
- [25] van Koningsveld M, van der Werff S, Jiang M, Lansen A, de Vriend H. Part IV ch 5 performance of ports and waterway systems. In: Koningsveld M, Verheij H, Taneja P, de Vriend H, editors. Ports and waterways. Netherlands: TU Delft OPEN Publishing; 2021, p. 433–58.
- [26] Jiang M, Baart F, Visser K, Hekkenberg R, Van Koningsveld M. Corridor Scale Planning of Bunker Infrastructure for Zero-Emission Energy Sources in Inland Waterway Transport. In: Proceedings of PIANC smart rivers 2022. Singapore: Springer Nature Singapore; 2023, p. 334–45. http://dx.doi.org/10.1007/978-981-19-6138-0\_30.
- [27] Jiang M, Baart F, Van Koningsveld M. OpenTNSim-Energy (v1.0.0). 2022, http://dx.doi.org/10.5281/zenodo.7098068.
- [28] van Koningsveld M, den Uijl J. OpenTNSim (v1.0.0). 2020, http://dx.doi.org/ 10.5281/zenodo.3813871.
- [29] Holtrop J, Mennen G. An approximate power prediction method. Int Ship-build Prog 1982;29(335). URL http://resolver.tudelft.nl/uuid:ee370fed-4b4f-4a70-af77-e14c3e692fd4.
- [30] Zeng Q, Thill C, Hekkenberg R, Rotteveel E. A modification of the ITTC57 correlation line for shallow water. J Mar Sci Technol 2019;24:642–57. http: //dx.doi.org/10.1007/s00773-018-0578-7.
- [31] Holtrop J. A statistical re-analysis of resistance and propulsion data. Int Shipbuild Prog 1984;31(363). URL https://api.semanticscholar.org/CorpusID:111508867.
- [32] Karpov A. Calculation of ship resistance in restricted waters. 1946, TRUDY GII. T. IV, 2. (in Russian).
- [33] van Terwisga T. Weerstand en voortstuwing van bakken: een literatuurstudie. MARIN Rep 49199-1-RD, Wagening Neth 1989.

- [34] Pompée P-J. About modelling inland vessels resistance and propulsion and interaction vessel-waterway: Key parameters driving restricted/shallow water effects. In: SMART RIVERS 2015. Buenos Aires, Argentina: Voies Navigables de France; 2015, p. 1–10.
- [35] Anku R, Pruyn J, Thill C. A review of the state-of-the-art sustainable and climateresilient inland waterway vessels. In: Proceedings of the international marine design conference. IMDC, 2024, http://dx.doi.org/10.59490/imdc.2024.826.
- [36] ITTC. ITTC 2013 Recommended Procedures: Resistance Uncertainty Analysis, Example for Resistance Test. Int Towing Tank Conf Venice Italy 2002.
- [37] Katsui T, Asai H, Himeno Y, Tahara Y. The proposal of a new friction line. In: Proceedings 5th Osaka Colloquium on Advanced Research on Ship Viscous Flow and Hull Form Design by EFD and CFD Approaches, Osaka, Japan. Osaka, Japan; 2005. p. 76–83.
- [38] Kim K, Roh G, Kim W, Chun K. A Preliminary Study on an Alternative Ship Propulsion System Fueled by Ammonia: Environmental and Economic Assessments. J Mar Sci Eng 2020;8(3). http://dx.doi.org/10.3390/jmse8030183.
- [39] Ligterink N, van Gijlswijk R, Kadijk G, Vermeulen R, Indrajuana A, Elstgeest M, et al. Emissiefactoren wegverkeer Actualisatie 2019. TNO report R10825v2, Den Haag, Netherlands: TNO; 2019,
- [40] Hulskotte J. EMS-protocol Emissies door Binnenvaart: Verbrandingsmotoren. TNO - Department of Climate Air and Sustainability report - version 4, Taskgroup Traffic and Transport, TNO - Department of Climate Air and Sustainability report - version 4; 2018.
- [41] Barrass C. Chapter 17 ship squat in open water and in confined channels. In: Barrass C, editor. ship design and performance for masters and mates. Oxford: Butterworth-Heinemann; 2004, p. 148–63. http://dx.doi.org/10.1016/B978-075066000-6/50019-2, URL https://www.sciencedirect.com/science/article/nii/B9780750660006500192.
- [42] European Commission TEN-T revision 2024 Annex III: European Transport Corridors. 2024, https://transport.ec.europa.eu/document/download/38f19f4b-50e8-4558-a5b9-fbd089a90349\_en?filename=TEN-T-guidelines-2024-annex-3.pdf. (Accessed 03 December 2024).
- [43] Schweighofer J, Suvačarov A. Evaluation of the fuel-consumption-reduction potential of a Danube vessel. In: 7th Transport Research Arena TRA. Vienna, Austria, 2018, http://dx.doi.org/10.5281/zenodo.1451695.
- [44] Schweighofer J, CaptBSzalma. Evaluation of a one-year operational profile of a danube vessel. In: PIANC World Congress. San Francisco, The United States of America, 2014, p. 1–12, URL https://www.researchgate.net/publication/ 266088659\_EVALUATION\_OF\_A\_ONE-YEAR\_OPERATIONAL\_PROFILE\_OF\_A\_ DANUBE VESSEL.
- [45] Salameh Z. Chapter 4 Energy Storage. In: Renewable energy system design. Boston, The United States of America: Academic Press; 2014, p. 201–98. http://dx.doi.org/10.1016/B978-0-12-374991-8.00004-0.
- [46] Bilen B, Zerjal M. An Optimized Propulsive and Manoeuvring System for River Pushboats. In: Proceedings of international conference on coastal ships and inland waterways. London, United Kingdom: Royal Institution of Naval Architects; 1999, p. 1–18.
- [47] Simić A, Radojcic D. On Energy Efficiency of Inland Waterway Self-Propelled Cargo Vessels. FME Trans 2013;41 No.2:138–45, URL https://www.mas.bg.ac. rs/istrazivanje/fme/vol41.
- [48] CBS. Pump prices motor fuels; location petrol station, type fuel. 2024, URL https://www.cbs.nl/en-gb/figures/detail/81567ENG. (Accessed 30 November 2024).
- [49] Viadonau Transport, Innovation, and Technology for the preservation and developmet of the Danube Waterway. 2024, https://www.viadonau.org/en/home. (Accessed 01 December 2024).
- [50] Yang Y, Tu H, Song L, Chen L, Xie D, Sun J. Research on Accurate Prediction of the Container Ship Resistance by RBFNN and Other Machine Learning Algorithms. J Mar Sci Eng 2021;9(4). http://dx.doi.org/10.3390/jmse9040376.
- [51] Gkioka D. Investigation of the power estimation for inland barges (Ph.D. thesis), Delft, The Netherlands: Delft University of Technology Faculty of Civil Engineering and Geosciences; 2023, URL https://resolver.tudelft.nl/uuid: a78922f9-beee-48bf-8a17-35baa138ad63.
- [52] Regulation (EU) 2016/1628 of the European Parliament and of the Council on requirements relating to gaseous and particulate pollutants from internal combustion engines for non-road mobile machinery. Off J Eur Union, L252/53 2016-09-14. URL https://eur-lex.europa.eu/legal-content/EN/TXT/PDF/ ?uri=CELEX:32016R1628.
- [53] Port of Rotterdam Authority. Port of rotterdam tariff book 2022. 2022, Contains differentiated port dues based on engine emission performance, including CCR2 surcharges and Green Award discounts. Official tariff regulations. URL https://www.portofrotterdam.com/sites/default/files/port-ofrotterdam-tariff-book-2022.pdf.
- [54] Wettengel J. Germany2019s carbon pricing system for transport and buildings. 2024, URL https://www.cleanenergywire.org/factsheets/germanys-plannedcarbon-pricing-system-transport-and-buildings. (Accessed 30 November 2024).
- [55] Dutch Emissions Authority Tarieven CO2-heffing. 2024, https://www. emissieautoriteit.nl/onderwerpen/tarieven-co2-heffing. (Accessed 11 October 2024).